

Title	Strain effects in wurtzite BN: elastic constants, internal strain and deformation potentials from hybrid functional density functional theory
Authors	Sheerin, Thomas P.;Schulz, Stefan
Publication date	2022-03-18
Original Citation	Sheerin, T. P. and Schulz, S. (2022) 'Strain effects in wurtzite BN: elastic constants, internal strain and deformation potentials from hybrid functional density functional theory', Physica Status Solidi - Rapid Research Letters. doi: 10.1002/pssr.202200021
Type of publication	Article (peer-reviewed)
Link to publisher's version	10.1002/pssr.202200021
Rights	© 2022, John Wiley & Sons Inc. This is the accepted version of the following item: Sheerin, T. P. and Schulz, S. (2022) 'Strain effects in wurtzite BN: elastic constants, internal strain and deformation potentials from hybrid functional density functional theory', Physica Status Solidi - Rapid Research Letters, doi: 10.1002/pssr.202200021, which has been published in final form at: https://doi.org/10.1002/pssr.202200021 . This article may be used for non-commercial purposes in accordance with Wiley Terms and Conditions for Use of Self-Archived Versions.
Download date	2024-05-16 14:07:05
Item downloaded from	https://hdl.handle.net/10468/12966

Strain effects in wurtzite BN: elastic constants, internal strain and deformation potentials from hybrid functional density functional theory

Thomas P. Sheerin*, Stefan Schulz

Thomas P. Sheerin

Department of Physics, University College Cork, Cork T12 YN60, Ireland

Email Address: 116352193@umail.ucc.ie

Thomas P. Sheerin, Stefan Schulz

Tyndall National Institute, Lee Maltings, Dyke Parade, Cork T12 R5CP, Ireland

Keywords: *Wurtzite boron nitride, hybrid density functional theory, HSE functional, deformation potentials, elastic constants, internal strain parameters*

Boron-containing III-nitride heterostructures have recently attracted significant attention for improving the efficiency of visible and UV light emitters. However, the fundamental material properties of wurtzite BN are largely unexplored. Here, highly accurate first principles calculations are used to gain insight into internal strain, elastic constants and electronic band structure deformation potentials. These parameters are key ingredients for simulating, and thus predicting, electronic and optical properties of boron-containing III-nitride-based light emitters. The ab initio calculations show, for instance, that the quasi-cubic approximation for deformation potentials is a poor approximation for wurtzite BN.

1 Introduction

Controlling, tailoring and engineering the crystal phase of semiconductor materials has received strong interest in recent years^[1, 2]. From the perspective of fundamental physics, crystal phase controlled heterostructures are ideal candidates for demonstrating quantum effects (e.g. the Aharonov-Bohm effect of excitons^[1]). These all-binary quantum structures exhibit flat interfaces and the absence of alloy fluctuations^[1]. In addition, changing the crystal phase of a material may allow for changing its fundamental properties. For instance, as demonstrated in Ref.^[2], while Ge is an indirect bandgap material in the cubic (diamond) phase it becomes a *direct* gap material in the hexagonal (lonsdaleite) phase. This finding is highly attractive for silicon photonic device applications. Overall, to drive the understanding of fundamental properties but also to design future devices, theoretical modelling is an essential ingredient. Here, density functional theory (DFT) plays an important role, since (i) it can provide insight into the fundamental material properties from first principles and (ii) the insight obtained can form the basis and input for developing empirical atomistic^[3, 4] but also continuum-based^[5, 6] models that allow for simulating full device structures.

Here we present results from highly accurate hybrid DFT studies on the properties of wurtzite (WZ) BN. While BN preferentially crystallizes in the hexagonal (2D) or zincblende phase^[7], it has recently drawn attention for alloying WZ III-nitride semiconductors InN, GaN and AlN^[8, 9, 10, 11, 12, 13]. Despite the fact that bulk WZ BN is difficult to synthesize, several works have succeeded in incorporating small fractions of WZ BN (mainly up to 10%, with some exceptions of slightly larger

This article has been accepted for publication and undergone full peer review but has not been through the copyediting, typesetting, pagination and proofreading process, which may lead to differences between this version and the [Version of Record](#). Please cite this article as [doi: 10.1002/pssr.202200021](https://doi.org/10.1002/pssr.202200021).

values near 20%) into other WZ III-nitrides^[8, 10, 12, 13]. Using WZ BN in III-N materials is thus attractive for optimizing the efficiency of e.g. light emitting diodes operating in the visible^[9, 8] to ultraviolet^[12, 11] spectral range. Recent theoretical studies on WZ BN have mainly focused on the band gap, piezoelectric coefficients and band offsets^[14, 15]. But, to perform full device simulations using, e.g., continuum-based $\mathbf{k} \cdot \mathbf{p}$ models, parameters such as band gap deformation potentials and elastic constants are required. We provide insight into these properties, along with internal strain parameters, which are essential for developing atomistic force-field models.

2 Results and Discussion

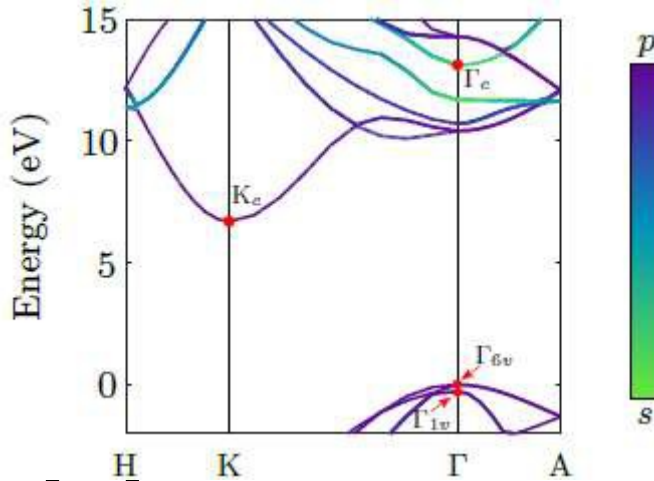
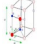


Figure 1: (Color online) The electronic band structure of wurtzite BN. The color-coding indicates the s - and p -orbital character of the different bands. Labels for selected states (K_c , Γ_c , Γ_{1v} , Γ_{6v}) important for deformation potential calculations, are also given.

All material parameters in this work are derived from highly accurate hybrid functional DFT calculations, using the projector-augmented wave method implemented in the plane-wave-based ab initio code VASP^[16, 17]. The plane-wave cutoff is set at 600 eV and a Γ -centred $8 \times 8 \times 8$ point mesh is used in all calculations. Here, we employ the Heyd-Scuseria-Ernzerhof (HSE) functional^[18] with a screening parameter of $\mu = 0.2$. To perform calculations for WZ BN, we use GaN as a starting point. In doing so, we first benchmark the outcome of our calculations with existing results for GaN from the literature before predicting data for WZ BN. Thus, we use the HSE exchange-mixing parameter to fit to the experimental bandgap of WZ GaN (3.51 eV^[19]); the resulting value ($\alpha = 0.284$, which is in good agreement with previous HSE-DFT studies^[20]) is then used for all WZ BN calculations, since the bandgap of WZ BN has not been conclusively determined experimentally. Figure 1 shows the obtained WZ BN band structure. Our calculations predict an indirect band gap of $E_g^K = E^{K_c} - E^{\Gamma_{6v}} = 13.71$ eV and a transition energy to Γ_c (see discussion below) of $E_g^{\Gamma_c} = E^{K_c} - E^{\Gamma_c} = 13.09$ eV, which are in good agreement with theoretical literature data^[15, 14].

Having considered the equilibrium electronic properties of WZ GaN and BN, we now proceed to obtain parameters that come into play when the crystal is strained. In this work, we focus on the deformation potentials a_c and D_p , the elastic constants C_{ij} and the internal strain parameters ζ_i . We begin with the deformation potentials. These parameters are key ingredients when calculating the electronic and optical properties of semiconductor heterostructures in the frame of semi-empirical atomistic approaches (e.g. tight-binding^[3]) or continuum-based models (like $\mathbf{k} \cdot \mathbf{p}$ theory^[5]). We note however that care must be taken when deriving deformation potentials from our DFT data, especially for use in $\mathbf{k} \cdot \mathbf{p}$ models. Since the WZ III-nitrides InN, GaN and AlN are *direct* gap

Defo. Pot. [eV]	GaN		BN	
	Present	Lit.	Present	Lit
$a_{cz} - D_1$	-6.03	-5.81	-2.36	–
$a_{ct} - D_2$	-8.98	-8.92	-24.44	–
D_3	5.38	5.47	2.71	3.90
D_4	-2.95	-2.98	-2.74	-3.32
	-2.80	-2.82	-4.05	-4.30
D_6	-3.95	-3.95	-6.42	–
ADPs				
a_{cz}	-8.60	–	-3.33	–
a_{ct}	-6.22	–	-21.42	–
D_1	-2.56	-20.0	-0.97	-19.2
D_2	2.76	-14.2	3.02	-14.0

The WZ BN and GaN deformation potentials obtained are summarized in Table 1. The GaN data show very good agreement with previously published HSE-DFT data, lending trust that the chosen approach should also provide highly accurate results for WZ BN. There exist no HSE-DFT literature data for the deformation potentials of BN and even for DFT within the local density approximation (LDA-DFT) the data are sparse (see e.g. Ref.^[26]); the inaccuracies of LDA-DFT in predicting electronic properties are well known and thus our HSE-DFT provides more accurate data, as well as data that were not available before (e.g. D_6 , $a_{cz} - D_1$ and $a_{ct} - D_2$). Overall, when comparing GaN and BN data, while most of the deformation potentials are similar in terms of sign and magnitude, $a_{ct} - D_2$ is almost a factor of 3 larger in BN. Such a large deformation potential can strongly affect the band edges in a heterostructure and thus the carrier confinement. However, the present approach does not allow us to distinguish if this will affect the conduction (a_c) or valence (D_v) band more strongly, since we only have access to $a_{ct} - D_2$. Determining the *absolute* deformation potential (ADPs) from DFT is challenging. To gain first insight into the ADPs, we use the $1s$ core level as the reference point for our energy scale and assume this level is independent of the applied strain. A detailed critical discussion of this approach can be found in Ref.^[27], but since we are aiming for first insights into the ADPs, this approach should be sufficient for our purposes.

The ADPs obtained for WZ BN and GaN are given in Table 1, along with literature data for comparison. Our values for the ADPs differ from those of Ref.^[26], e.g. we get different signs for D_2 . However, Ref.^[26] does not give information about the reference energy. It seems that the energy scale set by the electronic structure calculation is used- this is, however, not absolute. Thus, our results should give a more accurate first insight into the ADPs. We briefly note that for both $a_{cz} - D_1$ and $a_{ct} - D_2$ in BN, the CB accounts for most of the movement under strain.

In a further step, we study the validity of the quasi-cubic approximation (QCA), which is often applied^[28, 21] in studies of WZ III-N systems because not all deformation potentials may be known accurately from experiment or theory. The QCA results, for instance, in $D_3 + 2D_4 = 0$ and $D_3 + 4D_5 - \sqrt{2}D_6 = 0$. Using our calculated values, for GaN we find a value of -0.52 eV for $D_3 + 2D_4$, which is consistent with Ref.^[25]; for WZ BN this value is -2.77 eV, deviating significantly

from zero. Looking at $D_3 + 4D_5 - \sqrt{2}D_6$ which again should be zero, for GaN we obtain -0.23 eV but for BN it is -4.41 eV. All this shows that the QCA is a very poor approximation for WZ BN and highlights the importance of our highly accurate first-principles calculations. It is interesting to consider why WZ BN violates the QCA to a far greater extent than WZ GaN. We partly attribute this, as in Ref.[29], to deviations of BN from the ideal WZ structure. However, these deviations are slight, and GaN suffers similar deviations from ideality: the u -parameter of BN is, from Table 2, equal to the ideal of 0.375, but its c/a ratio is noticeably larger than the ideal $\sqrt{8/3}$ value; the reverse is true for GaN. As discussed in Ref.[29], further contributions to the breakdown of the QCA in WZ materials may arise from (strong) 3rd nearest-neighbor interactions. Indeed, the lattice constants of BN are $\sim 20\%$ smaller than those of GaN, and as a consequence one could expect stronger 3rd nearest-neighbor interactions in WZ BN than in WZ GaN, since the atoms are closer to each other.

To calculate the elastic properties, we use the stress-strain method, since in general this leads to a faster and smoother convergence with respect to k -point sampling and cutoff energy[30]. Choosing such an approach is particularly beneficial for the numerically demanding HSE-DFT framework used here. To determine the elastic constants C_{ij} , we employ the stress-strain relation:

$$\sigma_i = \sum_j C_{ij} \varepsilon_j, \quad (2)$$

where σ_i is the i th stress-tensor component and ε_j the j th strain-tensor component (Voigt notation). Subjecting the lattice to each of the four strain branches used for the deformation potentials above and extracting the strain tensor from VASP allows determination of the C_{ij} by fitting (again over the $\pm 2\%$ strain range).

Table 2: Independent elastic tensor components C_{ij} and bulk modulus B of WZ GaN and BN, along with lattice constants and u -parameter, as predicted by this work (“Present”). WZ BN literature (“Lit.”) data have been taken from Refs.^[26, 15, 31], while for GaN data from Refs.^[32, 19, 30] are given.

	GaN		BN	
		Lit.	Present	Lit.
C_{11} [GPa]	377	390	1016	982
C_{12} [GPa]	137	145	144	134
C_{13} [GPa]	92	106	64	74
C_{33} [GPa]	407	398	1113	1077
C_{44} [GPa]	103	105	361	388
B [GPa]	200	210	410	401
a [Å]	3.174	3.189	2.534	2.549
c [Å]	5.165	5.185	4.189	4.223
u	0.377	0.377	0.375	0.374

Table 1 summarizes our calculated elastic constants, including the bulk modulus B , for WZ GaN and BN. We also display the lattice constants and the u -parameter, and compare all data to the literature. Overall, for GaN we find very good agreement with the literature^[32]. For WZ BN, the agreement with the literature is also good. However, for C_{11} , C_{12} , and C_{33} our values are larger while C_{13} is lower compared to Ref.^[26], which uses LDA-DFT. It has already been discussed in the literature that HSE-DFT is in general superior to LDA calculations for predicting structural properties^[33]. Thus, our results are expected to be more accurate. Comparing the results for GaN and BN, we note that the diagonal components C_{ii} of the elastic tensor are a factor of order 3 larger in WZ BN. This is an important observation for c -plane WZ quantum wells (QWs), the “standard” structure for III-N based optoelectronic devices. In such a system, the strain along the c -axis can be approximated by $\epsilon_1 = -2(C_{13}/C_{33})\epsilon_1$, where ϵ_1 is the strain in the growth (c) plane given by $\epsilon_1 = (a_B - a_W)/a_W$, where a_W (a_B) is the well (barrier) in-plane lattice constant. Thus, given the much larger value of C_{33} and smaller value of C_{13} in BN when compared to GaN, the ratio C_{13}/C_{33} should reduce when adding BN to a GaN QW. Also, when considering a BGaN QW grown on AlN, the smaller lattice mismatch results in a reduction of ϵ_1 . This means that the overall strain in such a system will be smaller compared to GaN/AlN, in turn causing a reduction in the piezoelectric polarization field^[34], this should be highly beneficial for the radiative recombination rate in BGaN/AlN QWs. However, further studies are required to gain insight into this question.

Finally, to determine the internal strain parameters we proceed largely as described in Ref.^[30]. Starting from the unstrained atomic positions of the two anions and cations in the WZ unit cell (see Figure 2), we apply strain to the lattice so that the positions become^[30]

$$\begin{aligned} \mathbf{r}^A &= \mathbf{r}_0^A, \\ \mathbf{r}^B &= (\mathbf{I} + \epsilon) \mathbf{r}_0^B + \mathbf{t}_1, \\ \mathbf{r}^C &= (\mathbf{I} + \epsilon) \mathbf{r}_0^C + \mathbf{t}_2, \\ \mathbf{r}^D &= (\mathbf{I} + \epsilon) \mathbf{r}_0^D + \mathbf{t}_3, \end{aligned} \quad (3)$$

where \mathbf{r}_0^A , \mathbf{r}_0^B , \mathbf{r}_0^C and \mathbf{r}_0^D denote the unstrained atomic positions, \mathbf{I} is the 3×3 identity, ϵ the strain tensor and \mathbf{t}_i the internal strain displacement vectors. Since we use different coordinates to Ref.^[30], each \mathbf{t}_i is given by $\mathbf{t}_i = \mathbf{R} \mathbf{t}'_i$, where \mathbf{R} is the change-of-basis matrix and \mathbf{t}'_i is found from Equation (9) of Ref.^[30] using the basis-transformed strain tensor, $\epsilon' = \mathbf{R}^{-1} \epsilon \mathbf{R}$, i.e.

$$\begin{aligned} \mathbf{t}'_1 &= c \left[\frac{\zeta_1 \epsilon'_1 + \zeta_5 \epsilon'_6}{2}, \frac{\zeta_1 \epsilon'_4 + \zeta_5 (\epsilon'_1 - \epsilon'_2)}{2}, \zeta_2 (\epsilon'_1 + \epsilon'_2) - \zeta_3 \epsilon'_3 \right], \\ \mathbf{t}'_2 &= c \left[-\frac{\zeta_4 \epsilon'_6}{2}, -\frac{\zeta_4 (\epsilon'_1 - \epsilon'_2)}{2}, 0 \right], \\ \mathbf{t}'_3 &= \mathbf{t}'_1 + \mathbf{t}'_2 - c \left[\zeta_5 \epsilon'_6, \zeta_5 (\epsilon'_1 - \epsilon'_2), 0 \right] \end{aligned} \quad (4)$$

We obtain the internal strain parameters ζ_i ($i = 1 - 5$) by applying the four strain branches from before and fitting to the above expressions.

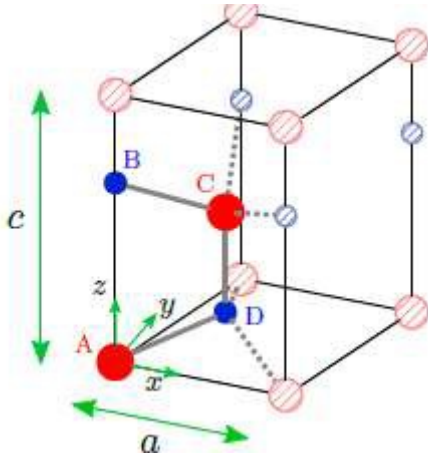


Figure 2: (Color online) The unit cell used in this study for the WZ crystal structure. Red (blue) denotes cations (anions), and stripe-filled circles belong to adjacent unit cells.

In all our calculations we constrain the internal displacements of the ions in the unit cell to conform to the symmetry of the WZ crystal, similar to Ref.[30]. This minimizes the impact of any numerical error of the finite k -point sampling. We observe that this symmetry-constraining has almost no effect on the deformation potentials and elastic constants, but is important for ζ_1 , ζ_4 and ζ_5 . The internal strain parameters obtained are shown in Table 3. For GaN we find very good agreement with previously published results, except for ζ_5 . In general, since ζ_1 , ζ_4 and ζ_5 are determined from strain branches that break the original C_{6v} WZ symmetry to smaller groups, they are quite sensitive to fine details of the calculation, like whether or not one uses the “symmetry constraining” mentioned above. Presumably, we and Ref.[30] use somewhat different settings in our calculations, which can explain the deviations in ζ_5 . The exact origin of the sensitivity in ζ_1 , ζ_4 and ζ_5 is an important topic but beyond the scope of this work. A comparison with the literature is not possible for WZ BN since there are no previously published data. An accurate theoretical determination of the internal strain parameters is important for three reasons. Firstly, it is experimentally not possible to determine these parameters with approaches currently available. Secondly, internal strain parameters ζ_i provide input to, but also a way to benchmark semi-empirical interatomic potentials [6]. Thirdly, internal strain parameters are tightly linked to local polarization effects in III-N materials, which in turn can lead to strong carrier localization effects [3, 35]. Comparing WZ GaN and BN, we find that the internal strain parameters ζ_i are much smaller in BN. This means the shift in the atomic positions is mainly determined by the macroscopic strain, so local piezoelectric effects and contributions to carrier localization effects may be reduced.

Table 3: The (dimensionless) internal strain parameters ζ_i of WZ GaN and BN (“Present”), as predicted in this work. GaN literature data are also given^[30] (“Lit.”).

ζ_i	GaN		BN
	Present	Lit.	Present
ζ_1	0.155	0.156	0.051
ζ_2	0.082	0.083	0.015
ζ_3	0.156	0.159	0.007
ζ_4	0.199	0.201	0.049
ζ_5	0.097	0.141	0.051

3 Conclusion

In summary, by using highly accurate first principles calculations, we provide insight into internal strain, elastic constants and electronic band structure deformation potentials of WZ BN. This material has attracted significant attention as a potential candidate to improve the efficiency of III-N-based devices. The parameters determined are key ingredients for simulating, and thus predicting, electronic and optical properties of boron-containing III-N light emitters. Our calculations show, for instance, that the QCA for deformation potentials is a poor approximation for WZ BN, highlighting the need for and importance of our accurate DFT study.

Acknowledgements

This work received funding from the Sustainable Energy Authority of Ireland and the Science Foundation Ireland (Nos. 17/CDA/4789 and 12/RC/2276 P2).

Conflict of Interest

The authors declare no conflict of interest.

Data Availability Statement

The data that support the findings of this study are available from the corresponding author upon reasonable request.

References

- [1] P. C. Sfir, O. Marquardt, R. B. Lewis, C. Sinito, M. Ramsteiner, A. Trampert, U. Jahn, L. Geelhaar, O. Brandt, V. M. Fomin, *Adv. Mater.* **2019**, *31* 1805645.
- [2] E. M. T. Madaly, A. Dijkstra, J. R. Suckert, D. Ziss, M. A. J. van Tilburg, C. Mao, Y. Ren, V. T. van Lange, K. Korzun, S. Kölling, M. A. Verheijen, D. Busse, C. Rödl, J. Furthmüller, F. Bechstedt, J. Stungl, J. J. Finley, S. Botti, J. E. M. Haverkort, E. P. A. M. Bakkers, *Nature* **2020**, *580* 205.
- [3] M. A. Caro, S. Schulz, E. P. O'Reilly, *Phys. Rev. B* **2013**, *88* 214103.
- [4] M. Łopuszynski, J. A. Majewski, *J. Phys.: Condens. Matter* **2010**, *22* 205801.
- [5] O. Marquardt, M. A. Caro, T. Koprucki, P. Mathe, M. Willatzen, *Phys. Rev. B* **2020**, *101* 235147.
- [6] E. J. O'Halloran, C. A. Broderick, D. S. P. Tanner, S. Schulz, E. P. O'Reilly, *Opt. Quant. Electron.* **2019**, *51* 314.

[7] V. L. Solozhenko, V. Z. Turkevich, W. B. Holzapfel, *J. Phys. Chem. B* **1999**, *103* 2903.

[8] S. Gautier, G. Orsal, T. Moudakir, N. Maloufi, F. Jomard, M. Alnot, Z. Djebbour, A. A. Sirenko, M. Abid, K. Pantzas, I. T. Ferguson, P. L. Voss, A. Ougazzaden, *J. Cryst. Growth* **2010**, *312* 641.

[9] L. Williams, E. Kioupakis, *Appl. Phys. Lett.* **2017**, *111* 211107.

[10] B. P. Gunning, M. W. Moseley, D. D. Koleske, A. A. Allerman, S. R. Lee, *J. Cryst. Growth* **2017**, *467* 130.

[11] R. C. Cramer, B. Bonef, J. English, C. E. Dreyer, C. G. Van de Walle, J. S. Speck, *J. Vac. Sci. Technol. A* **2017**, *35* 041509.

[12] X. Li, S. Sundaram, Y. El-Gmili, T. Moudakir, F. Genty, S. Bouchoule, G. Patriache, R. D. Dupuis, P. L. Voss, J.-P. Salvestrini, A. Ougazzaden, *Phys. Status Solidi A* **2015**, *212* 745.

[13] X. Li, S. Sundaram, Y. El-Gmili, F. Genty, S. Bouchoule, G. Patriache, P. Disseix, F. Réveret, J. Leymarie, J.-P. Salvestrini, R. D. Dupuis, P. L. Voss, A. Ougazzaden, *J. Cryst. Growth* **2015**, *414* 119.

[14] M. E. Turiansky, J.-X. Shen, D. Wickramaratne, C. G. Van de Walle, *J. Appl. Phys.* **2019**, *126* 095706.

[15] C. E. Dreyer, J. L. Lyons, A. Janotti, C. G. Van de Walle, *Appl. Phys. Express* **2014**, *7* 031001.

[16] G. Kresse, J. Furthmüller, *Phys. Rev. B* **1996**, *54* 11169.

[17] G. Kresse, D. Joubert, *Phys. Rev. B* **1999**, *59* 1758.

[18] J. Heyd, G. E. Scuseria, M. Ernzerhof, *J. Chem. Phys.* **2003**, *118* 8207.

[19] I. Vurgaftman, J. R. Meyer, *J. Appl. Phys.* **2003**, *94* 3675.

[20] P. G. Moses, M. Miao, Q. Yan, C. G. Van de Walle, *J. Chem. Phys.* **2011**, *134* 084703.

[21] S. L. Chuang, C. S. Chang, *Phys. Rev. B* **1996**, 56 2491.

[22] B. P. Gunning, M. W. Moseley, D. D. Koleske, A. A. Allerman, S. R. Lee, *J. Cryst. Growth* **2017**, 464 190.

[23] J.-X. Shen, D. Wickramaratne, C. G. Van de Walle, *Phys. Rev. Mat.* **2017**, 1 065001.

[24] O. Yan, P. Rinke, M. Scheffler, C. G. Van de Walle, *Appl. Phys. Lett.* **2009**, 95 121111.

[25] Q. Fan, P. Rinke, M. Scheffler, C. G. Van de Walle, *Appl. Phys. Lett.* **2010**, 97 181102.

[26] K. Shimada, T. Sota, K. Suzuki, *J. Appl. Phys.* **1998**, 84 4951.

[27] A. Janotti, C. G. Van de Walle, *Phys. Rev. B* **2007**, 75 121201(R).

[28] G. Benbach, M. Feneberg, M. Röppischer, C. Werner, N. E. C. Cobet, T. Meisch, K. Thonke, A. Dadgar, J. Bläsing, A. Krost, R. Goldhahn, *Phys. Rev. B* **2011**, 83 195202.

[29] H. Ebukura, K. Kamiya, K. Shiraishi, A. A. Yamaguchi, *Phys. Status Solidi C* **2011**, 8 2279.

[30] M. A. Caro, S. Schulz, E. P. O'Reilly, *Phys. Rev. B* **2012**, 86 014117.

[31] A. Nagakubo, H. Ogi, H. Sumiya, K. Kusakabe, M. Hirao, *Appl. Phys. Lett.* **2013**, 102 241909.

[32] A. Polian, M. Grimsditch, I. Grzegory, *J. Appl. Phys.* **1996**, 79 3343.

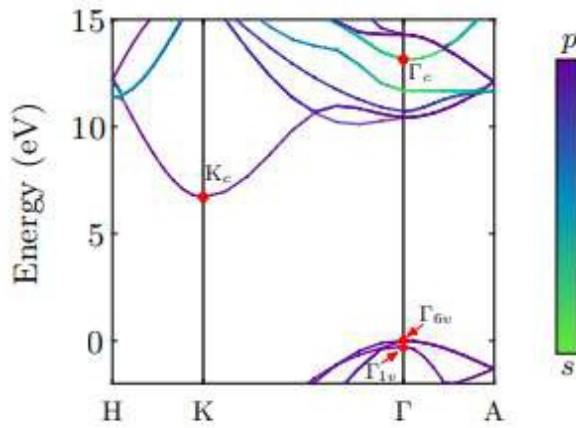
[33] D. S. P. Tanner, S. S. M. A. Caro, E. P. O'Reilly, *Phys. Rev. Materials* **2019**, 3 013604.

[34] M. A. Caro, S. Schulz, S. B. Healy, E. P. O'Reilly, *J. Appl. Phys.* **2011**, 109 084110.

[35] T. P. Sheerin, D. S. P. Tanner, S. Schulz, *Phys. Rev. B* **2021**, 103 165201.

Table of Contents text

The deformation potentials, elastic constants and internal strain parameters of wurtzite (WZ) BN are determined using hybrid density functional theory. WZ BN is a promising material for optimizing the efficiency of III-nitride-based devices, and these parameters are essential input for modelling of such systems. The results also show e.g. that the quasi-cubic approximation is very inaccurate for WZ BN.



ToC Figure

Accepted